

Physics objects for top physics in CMS

JYOTHSNA RANI KOMARAGIRI¹

on behalf of the CMS collaboration

Affiliation:

*Centre for High Energy Physics,
Indian Institute of Science, Bangalore - 560012, India*

E-mail: jyothsna@cern.ch

We present the status and performance of the physics objects with data corresponding to an integrated luminosity of 12.9 fb^{-1} collected at 13 TeV by the CMS experiment. We cover the performance of the physics objects extensively used in physics analyses involving top quarks.

PRESENTED AT

*9th International Workshop on Top Quark Physics,
Olomouc, Czech Republic, September 19–23, 2016*

¹Speaker

1 Introduction

The Large Hadron Collider (LHC) is providing proton-proton collisions at an unprecedented center-of-mass energy of $\sqrt{s} = 13$ TeV with the start of Run 2 in 2015. The collision data recorded by the Compact Muon Solenoid (CMS) [1] experiment reopen the opportunity to search for new physics phenomena at the TeV scale and to perform precision measurements of the standard model at a higher center-of-mass energy. To carry out these searches and precision measurements we need to understand our detector and the performance of various physics objects at higher center-of-mass energy as well as varying running conditions (high pile up, increasing instantaneous luminosity). The decay products from a top quark contain most of the physics objects we identify in our detector. We present the performances of all physics objects used in the physics analyses involving top quarks.

2 Event Reconstruction

Stable particles are identified with the Particle Flow (PF) algorithm [2] that reconstructs each individual particle with an optimized combination of information from the various elements of the CMS detector. The energy of photons is directly obtained from the ECAL measurement, corrected for zero-suppression effects. The energy of electrons is determined from a combination of the electron momentum at the primary interaction vertex as determined by the tracker, the energy of the corresponding ECAL cluster, and the energy sum of all bremsstrahlung photons spatially compatible with originating from the electron track. The energy of muons is obtained from the curvature of the corresponding track. The energy of charged hadrons is determined from a combination of their momentum measured in the tracker and the matching ECAL and HCAL energy deposits, corrected for zero-suppression effects and for the response function of the calorimeters to hadronic showers. Finally, the energy of neutral hadrons is obtained from the corresponding corrected ECAL and HCAL energy.

3 Jets and Missing Transverse Energy

Jets are reconstructed by clustering PF particles using the anti-kT (AK) jet clustering algorithm, with a distance parameter $R = 0.4$ (AK4 jets). For the boosted topologies, jets are clustered with a larger opening angle corresponding to $R = 0.8$ (AK8 jets). When clustering the particles in jets, isolated electrons and muons as well as charged particles associated with other interaction vertices are removed. Jet momentum is determined as the vectorial sum of all particle momenta in the jet. Jet energies are calibrated to correct for the different detector response as a function of the transverse momentum and pseudorapidity of the jets. Furthermore, an offset

correction is applied to jet energies to take into account the contribution from additional proton-proton interactions within the same bunch crossing. Comparison of jet response dependency on the jet p_T in data and simulation is shown Figure 1 (left). Jet energy corrections and resolution can be found in Ref. [3].

The default missing transverse energy in the transverse plane (MET) is reconstructed by the vector sum of all particle-flow particles in the opposite direction. Performance of 2016 cleaning algorithms on missing transverse energy distribution is shown in Figure 1 (right). More details and performance of MET algorithms can be found in Ref. [4].

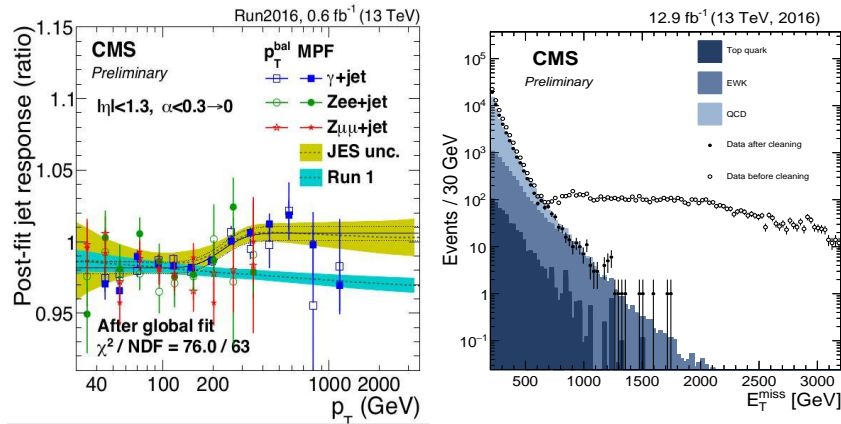


Figure 1: Data and simulation comparison for the jet response dependency on the jet p_T (left). The MissingET distributions for events passing the dijet selection with the 2016 cleaning algorithms applied including the one based on jet identification requirements (filled markers), without the 2016 cleaning algorithms applied (open markers), and from simulation (filled histograms) (right).

4 b tagging

Details about b tagging in CMS can be found in [5]. The Combined Secondary Vertex (CSVv2) tagger using multivariate technique based on track information and vertex information is the best performed algorithm in CMS. The other available taggers are Jet Probability (JP) tagger based on the track information and combined Multivariate Analysis (cMVAv2) tagger which makes use of track, vertex and soft lepton information using multivariate technique. The performance of the JP, CSVv2 and cMVAv2 taggers in simulated top pair production events is shown in Figure 2 (left). The performance of the b tagging algorithms has been measured using the data. The data and simulation comparisons can be found in Ref. [6].

We also have a c tagging algorithm for identifying jets originating from c -quarks. More details about c tagger along with its performance can be found in Ref. [8].

In boosted topologies b tagging can be performed applying the standard CSVv2 tagger to larger cone jets (known as fatjets) or to their subjets, obtained with substructure algorithms. A dedicated training has also been performed for fat jets originating from a boosted resonance decaying into a $b\bar{b}$ pair, outperforming the subjet and fatjet b tagging in such a topology, as shown in Figure 2 (right).

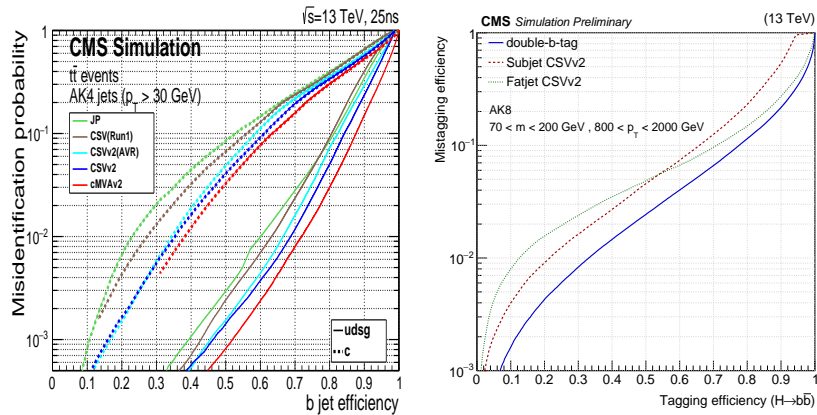


Figure 2: Performance of the b jet identification efficiency algorithms demonstrating the probability for non- b jets to be misidentified as b jet as a function of the efficiency to correctly identify b jets (left). Comparison of the performance of the double- b tagger, the minimum CSVv2 value among the two subjets b tag scores, and fat jet b tag which exploits CSVv2 algorithm (right).

5 Electrons

Electron reconstruction in Run2 is completely integrated with particle flow (PF) and provides additional flexibility at analysis level. As can be seen in Figure 3 (left) reconstructed $Z \rightarrow ee$ mass distribution using electron tuned energy corrections for barrel-barrel electron pairs shows good agreement between data and simulation. The efficiency for cut-based electron identification is measured with the tag and probe method and shown in five pseudorapidity ranges as a function of the electron transverse momentum and the results are shown Figure 3 (right). Other kinematics distributions of electrons are also compared between data and simulation and show a good agreement (see Ref. [9]).

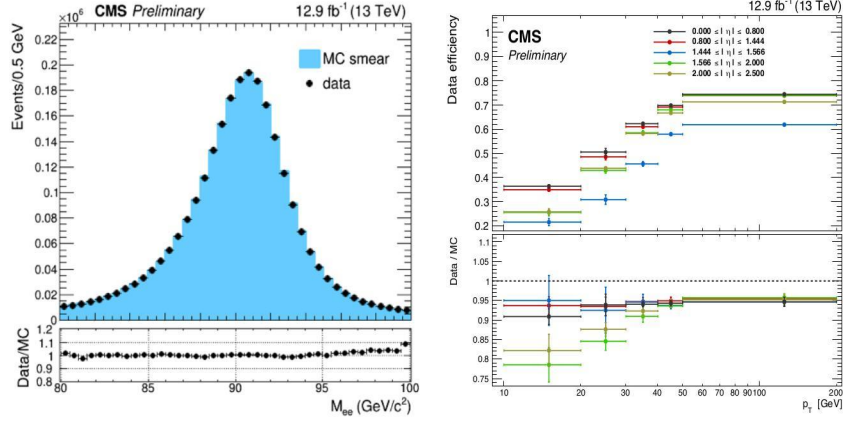


Figure 3: Data (black dots) and simulation (light blue) $Z \rightarrow ee$ mass distribution reconstructed with electron tuned energy corrections for barrel-barrel electron pairs (left). Electron identification efficiency in data (right top) and data to simulation efficiency ratios (right bottom) measured for the tight cut-based identification.

6 Muons

Efficiencies are computed by means of the tag-and-probe method exploiting $Z \rightarrow \mu\mu$ resonances. Computed identification and isolation efficiencies for tight working point as a function of probe muon p_T (left) and number of primary vertices (right) are shown in Figure 4. Good agreement between data and simulation can be seen. Other kinematics distributions of muons are also compared between data and simulation and show a good agreement (see Ref. [10]).

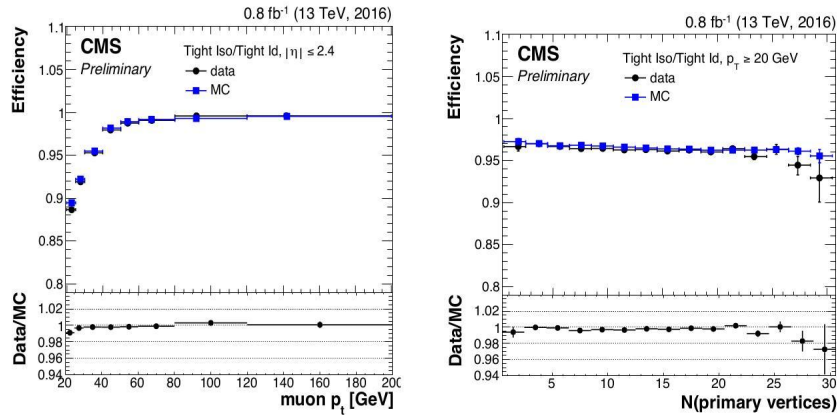


Figure 4: Muon identification and isolation efficiency for tight working points in shown as function of probe muon p_T (left) and number of primary vertexes (right).

7 Conclusions

The object performance study is the key for the measurements involving top quarks and also searches beyond the Standard Model. Performance of various physics objects extensively used in Top physics at CMS using RunII data shows good agreement between data and simulation.

References

- [1] CMS Collaboration, The CMS experiment at the CERN LHC, **JINST 3:S08004,2008**
- [2] CMS Collaboration, Particle-Flow Event Reconstruction in CMS and Performance for Jets, Taus and MET, **CMS-PAS-PFT-09-001**
- [3] CMS Collaboration, “Jet energy scale and resolution performances with 13TeV data”, **CMS-DP-2016-020**
- [4] CMS Collaboration, “Performance of missing energy reconstruction in 13 TeV pp collision data using the CMS detector”, **CMS-PAS-JME-16-004**
- [5] CMS Collaboration, “Identification of b quark jets at the CMS Experiment in the LHC Run 2”, **CMS-PAS-BTV-15-001**
- [6] CMS Collaboration, “Performance of b tagging Algorithms in Proton Collisions at 13 TeV using the 2016 Data”, **CMS-DP-2016-042**
- [7] CMS Collaboration, “Identification of double-b quark jets in boosted event topologies”, **CMS-PAS-BTV-15-002**
- [8] CMS Collaboration, “Identification of c-quark jets at the CMS experiment”, **CMS-PAS-BTV-16-001**
- [9] CMS Collaboration, “Electron and photon performance in CMS with first 12.9 fb⁻¹ of 2016 data”, **CMS-DP-2016-049**
- [10] CMS Collaboration, “Muon tag and probe efficiency on 2016 data”, **CMS-DP-2016-043**